J Mol Model (2010) 16:119–127
DOI 10.1007/s00894-009-0525-y

ORIGINAL PAPER

A theoretical study of red-shifting and blue-shifting hydrogen bonds occurring between imidazolidine derivatives and PEG/PVP polymers

Boaz G. Oliveira · Maria C. A. Lima · Ivan R. Pitta · Suely L. Galdino · Marcelo Z. Hernandes

Received: 27 February 2009 / Accepted: 9 April 2009 / Published online: 12 June 2009

Abstract A theoretical study is presented with the aim to investigate the molecular properties of intermolecular complexes formed by the monomeric units of polyvinylpyrrolidone (PVP) or polyethyleneglycol (PEG) polymers and a set of four imidazolidine (hydantoine) derivatives. The substitution of the carbonyl groups for thiocarbonyl in the hydantoin scaffold was taken into account when analyzing the effect of the hydrogen bonds on imidazolidine derivatives. B3LYP/6-31G(d,p) calculations and topological integrations derived from the quantum theory of atoms in molecules (QTAIM) were applied with the purpose of examining the N–H···O hydrogen bond strengths formed between the amide group of the hydantoine ring and the oxygen atoms of PVP and PEG polymers. The effects caused by the N–H···O interaction fit the typical evidence for hydrogen bonds, which includes a variation in the stretch frequencies of the N–H bonds. These frequencies were identified as being vibrational red-shifts because their values decreased. Although the values of such calculated interaction energies are between 12 and 33 kJ mol^{-1}, secondary intermolecular interactions were also identified. One of these secondary interactions is formed through the interaction of the benzyl hydrogen atoms with the oxygen atoms of the PVP and PEG structures. As such, we have analyzed the stretch frequencies on the C–H bonds of the benzyl groups, and blue-shifts were identified on these bonds. In this sense, the intermolecular systems formed by hydantoine derivatives and PVP/PEG monomers were characterized as a mix of red-shifting and blue-shifting hydrogen-bonded complexes.

Keywords Blue-shift · Imidazolidine · PEG · PVP · QTAIM · Red-shift

Electronic supplementary material The online version of this article (doi:10.1007/s00894-009-0525-y) contains supplementary material, which is available to authorized users.

B. G. Oliveira (✉) · M. Z. Hernandes
Departamento de Ciências Farmacêuticas,
Universidade Federal de Pernambuco,
50740-521 Recife, PE, Brazil
e-mail: boazgaldino@gmail.com

M. C. A. Lima · I. R. Pitta · S. L. Galdino
Departamento de Antibióticos,
Universidade Federal de Pernambuco,
50670-901 Recife, PE, Brazil

Introduction

It has been established that the chemical knowledge of biological systems at the molecular level is attributed to the careful study of various intermolecular interactions, such as hydrophobic, London dispersion forces, dipole polarizability and mainly, hydrogen bonds [1]. In drug design [2], the study of hydrogen bonds is often performed through virtual screening analysis or docking calculations [3–5]. However, recently, a great interest has been taken in studying the occurrence of hydrogen bonds in polymers [6–9], specifically those in solid dispersions widely used for pharmaceutical preparations [10, 11]. Along these lines of study, Sigalas *et al*. [12] have reported results regarding the release mechanism of felodipine (FLP) in solid dispersions by using polyvinylpyrrolidone (PVP) and polyethyleneglycol (PEG) polymers. Besides characterizing the optimized geometries for the FLP···PVP and FLP···PEG complexes, a discussion was undertaken regarding the formation of

specific hydrogen bonds between the proton donor of the N–H bond of the felodipine (FLP) and the carbonylic oxygen (PVP) or the ether oxygen atoms (PEG). Furthermore, Teberekidis and Sigalas [13] have also reported a detailed theoretical work of the structures and related phenomena for the FLP···PVP and FLP···PEG complexes, and their results are in agreement with experimental data previously documented [12].

In terms of treatment for neglected diseases [14], it is widely known that hydantoine derivatives are an important class of compounds with anti-shistosomiasis and anticonvulsant activities [15, 16]. Hydantoin (imidazolidine-2,4-dione **1a**) is a 2,4-diketotetrahydroimidazole discovered by Baeyer in 1861 [17]. Thiohydantoins and their derivatives, however, were prepared as bioisosters of hydantoins with similar biological behavior. In biological medium, the pharmacokinetics of hydantoin derivatives in a sodium channel are barely influenced by their structural characteristics, such as the substitution of aromatic rings, acceptor sites and hydrogen bonding groups [18]. However, it is important to stress that hydantoine derivatives such as imidazolidine and thiazolidine, depending on their substituted groups, are known by their very limited solubility in aqueous medium, which induces the necessity of using dimethyl sulfoxide (DMSO) as a solvent in biological tests. In order to overcome this solubility problem, the preparation of solid dispersions, including drugs, in hydrophilic carriers (polymers like PVP and PEG, for example) is a widely used technique. Therefore, it would be of interest to verify the behavior of hydantoine derivatives **1a**, **2a**, **3a** and **4a** (Fig. 1) when they interact with monomeric units of polyvinylpyrrolidone (PVP) and polyethyleneglycol (PEG) polymers [19]. Such analysis will be carried out through a detailed characterization of hydrogen bonds, where the interaction strength for the (**1a-4a**)···PVP and (**1a-4a**)···PEG intermolecular complexes must be carefully investigated. The goal of this theoretical study is to gain information that could be used in future solid dispersion preparations of the hydantoine derivatives.

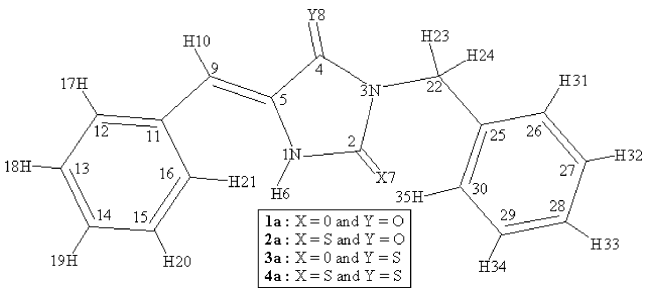

Fig. 1 Representation of the hydantoin ring skeletal structures studied in this work. 1a (imidazolidine–2,4-dione), 2a (2-thioxo-imidazolidin-4-one), 3a (4-thioxo-imidazolidin-2-one) and 4a (imidazolidine-2,4-dithione)

Thus, for this report, we proposed a theoretical study of the molecular parameters of the systems above using density functional theory (DFT) [20, 21] calculations. First, we focus on a detailed analysis of geometry and infrared spectrum, by emphasizing the intermolecular distances and changes in the electronic structure. Making reference to hydrogen-bonded complexes, it is well-established that the molecular changes mentioned above are related to an enhancement in the bond lengths of the proton donors [22–24]. From a geometric point of view and in terms of infrared spectrum, such changes are identified typically as red-shift effects, where the stretch frequencies of the proton donors are shifted downward in value, which is followed by an increase in their absorption intensities [25]. For this reason, a topological description of the electronic density will be achieved here by using the quantum theory of atoms in molecules (QTAIM) [26]. This theory should allow for the location of concentrations and depletions of charge density, along with their relationships to vibrational parameters, such as the red-shifts on proton donor bonds. Therefore, we hope to analyze the formation of the NH(**1a-4a**)···O (PVP or PEG) hydrogen bonds along with other secondary interactions, such as those formed between the carbonyl or thiocarbonyl groups of the hydantoine derivatives and the ethylenic hydrogen atoms of PVP or PEG. Currently, numerous studies regarding hydrogen-bonded complex structures have been reported, where the presence of secondary interactions [27–33] or new kinds of hydrogen bonds formed by multiple proton-acceptor centers have been demonstrated [34–37]. In this study, we have invested efforts to identify and characterize all intermolecular interactions on NH(**1a**–**4a**)···O (PVP or PEG) complexes, including hydrogen bonds or blue-shifting ones.

Computational methods

The optimized geometries of the (**1a**–**4a**)···PVP and (**1a**–**4a**)···PEG complexes were obtained at the B3LYP/6–31G(d,p) level of theory, where all calculations were performed in the GAUSSIAN 03 W program [38]. There have been previous reports, including a large number of computational studies, about hydrogen-bonded complexes where DFT functionals have been successfully applied [39, 40]. Thus, we chose the B3LYP as our standard hybrid. Moreover, we used the 6–31G(d,p) basis set because it has been considered accurate for predicting molecular properties of polymers [41] in addition to hydrogen bond interactions. All QTAIM topological calculations were executed using the GAUSSIAN 03 W program, according to the protocol implemented by Cioslowski [42–44]. In addition, some complementary electronic integrations were processed with the AIM 2000 1.0 program [45].

The values of the binding energies (ΔE) were determined according to the supermolecule approach [46], as follows:

$$\Delta E = E(\text{Hydrogen Complex}) - \sum [E(\text{IsolatedMolecules})]. \quad (1)$$

Results of the binding energies, ΔE, were corrected by the zero point energy (ZPE) [47] values and by Boys and Bernardi's Basis sets superposition error (BSSE) [48] calculations. Finally, each value of corrected interaction energy ΔE^C was obtained with the equation (2):

$$\Delta E^c = \Delta E - \Delta ZPE - BSSE. \quad (2)$$

Results and discussion

Geometry

From B3LYP/6–31G(d,p) calculations, the values of the most important intermolecular and intramolecular distances of the PVP···**1a** (I), PVP···**2a** (II), PVP···**3a** (III), PVP···**4a** (IV), PEG···**1a** (V), PEG···**2a** (VI), PEG···**3a** (VII) and PEG···**4a** (VIII) complexes are listed in Table 1. If we consider these results, it is natural to conclude that all these interactions are hydrogen bonds because at these distances values in range of 1.823–3.426 Å are shorter than the sum of the van der Waals radii [49] for the respective atoms involved.

Structurally, it is important to consider that the main criterion used to measure the hydrogen bond strength is the perturbation of the molecular properties on the monomers after formation of the complex. As an example, we chose two intermolecular systems to be evaluated, the (I) and (V) complexes. By analyzing the values of the $R(O_{36}\cdots H_6)$ and the $R(O_{38}\cdots H_6)$ hydrogen bond distances, we can observe that complex (I) is more strongly bonded than (V). Indeed, this tendency is verified in all the complexes (I-VIII), although in the case of (I) and (V), we must emphasize that other secondary hydrogen bonds could be observed. Besides the $(O_{36}\cdots H_6)$ and $(O_{38}\cdots H_6)$ interactions, the $(O_{36}\cdots H_{21})$ and $(O_{38}\cdots H_{21})$ contacts seem to be chemically functioning as hydrogen bonds on complexes (I) and (V). Moreover, the existence of multiple hydrogen bonds on

Table 2 Main structural changes in (**1a**), (**2a**), (**3a**) and (**4a**) monomers upon the formation of the PVP···**1a** (I), PVP···**2a** (II), PVP···**3a** (III), PVP···**4a** (IV), PEG···**1a** (V), PEG···**2a** (VI), PEG···**3a** (VII) and PEG···**4a** (VIII) complexes using B3LYP/6-31G (d,p) calculations

Molecular systems	Main structural changes			
	r(NH)	Δr(NH)	r(CH)	Δr(CH)
1a	1.0079	–	1.0853	–
2a	1.0078	–	1.0852	–
3a	1.0077	–	1.0852	–
4a	1.0079	–	1.0853	–
(I)	1.0257	0.0178	1.0824	−0.0028
(II)	1.0267	0.0189	1.0826	−0.0027
(III)	1.0259	0.0182	1.0818	−0.0035
(IV)	1.0269	0.0190	1.0821	−0.0032
(V)	1.0218	0.0139	1.0826	−0.0020
(VI)	1.0233	0.0155	1.0821	−0.0031
(VII)	1.0214	0.0137	1.0819	−0.0033
(VIII)	1.0233	0.0154	1.0815	−0.0038

* All r values are given in angstroms

Table 1 The set of important interaction distances in PVP···**1a** (I), PVP···**2a** (II), PVP···**3a** (III), PVP···**4a** (IV), PEG···**1a** (V), PEG···**2a** (VI), PEG···**3a** (VII) and PEG···**4a** (VIII) complexes using B3LYP/6-31G(d,p) calculations

H-Bonds	Hydrogen-bonded complexes				H-Bonds	Hydrogen-bonded complexes			
	(I)	(II)	(III)	(IV)		(V)	(VI)	(VII)	(VIII)
$R(O_{36}\cdots H_6)$	1.837	1.823	1.832	1.826	$R(O_{38}\cdots H_6)$	1.899	1.907	2.906	1.914
$R(O_{36}\cdots H_{21})$	2.309	2.223	2.281	2.190	$R(O_{38}\cdots H_{21})$	2.453	2.297	2.412	2.260
$R(H_{42}\cdots O_7)$	2.369	–	2.385	–	$R(H_{47}\cdots O_7)$	2.697	–	2.695	–
$R(H_{35}\cdots O_7)$	2.919	–	2.626	–	$R(H_{47}\cdots S_7)$	–	3.242	–	3.255
$R(H_{31}\cdots O_8)$	2.900	–	–	–	$R(H_{44}\cdots O_7)$	2.699	–	2.689	–
$R(H_{31}\cdots S_8)$	–	–	3.268	–	$R(H_{44}\cdots S_7)$	–	3.267	–	3.260
$R(H_{46}\cdots O_7)$	–	3.115	–	–	$R(H_{35}\cdots O_7)$	2.962	–	2.631	–
$R(H_{46}\cdots S_7)$	–	–	–	3.099	$R(H_{35}\cdots S_7)$	–	3.259	–	2.948
$R(S_8\cdots H_{23})$	–	2.627	–	2.933	$R(O_8\cdots H_{23})$	2.875	–	–	–
$R(H_{50}\cdots S_7)$	–	3.428	–	–	$R(O_8\cdots H_{31})$	–	2.637	–	–
$R(S_7\cdots H_6)$	–	–	–	3.415	$R(S_8\cdots H_{10})$	–	–	2.741	–
$R(S_7\cdots H_{24})$	–	–	–	2.988	$R(S_7\cdots H_{24})$	–	–	–	2.712
$R(S_8\cdots H_{10})$	–	–	–	2.708					

* All R values are given in angstroms

complexes (I) and (V) has also been verified, including ($O_7\cdots H_{42}$) and ($O_7\cdots H_{44}$), which present distance values of 2.369 Å and 2.699 Å, respectively. For complex (V), the distance value of 2.962 Å for the ($O_7\cdots H_{35}$) interaction also indicates the formation of an intramolecular hydrogen bond.

The most important structural evidence for the formation of hydrogen complexes is the enhanced bond lengths of the proton donors. According to the values listed in Table 2, one can see that the Δr(NH) and Δr(CH) values indicate an increase and a decrease of the NH and CH bond lengths on the imidazolidinic derivatives, respectively. It is important to pay special attention to the hydrogen bonds ($O_{36}\cdots H_6$) and ($O_{36}\cdots H_{21}$) for complex (I) (see Fig. 2). Nevertheless, we should mention that enlarging the NH bond length is an indication of the vibrational red-shifts on this bond. Naturally, this information is one of the most important pieces of evidence for the identification of hydrogen-bonded complexes, although the shortening of the CH bond length is indeed related to a non-typical type of intermolecular interaction known as an anti-hydrogen bond. More recently, this kind of interaction is called a blue-shifting hydrogen bond. However, it is important to emphasize that this definition was not given by a geometrical analysis, but instead, it was named by an interpretation of the infrared spectrum, allowing for a careful characterization of these effects on the NH and CH bonds.

Vibrational parameters

In Table 3, the main vibrational modes of the **1a**, **2a**, **3a** and **4a** isolated molecules are presented, along with complexes (I), (II), (III), (IV), (V), (VI), (VII) and (VIII). Essentially,

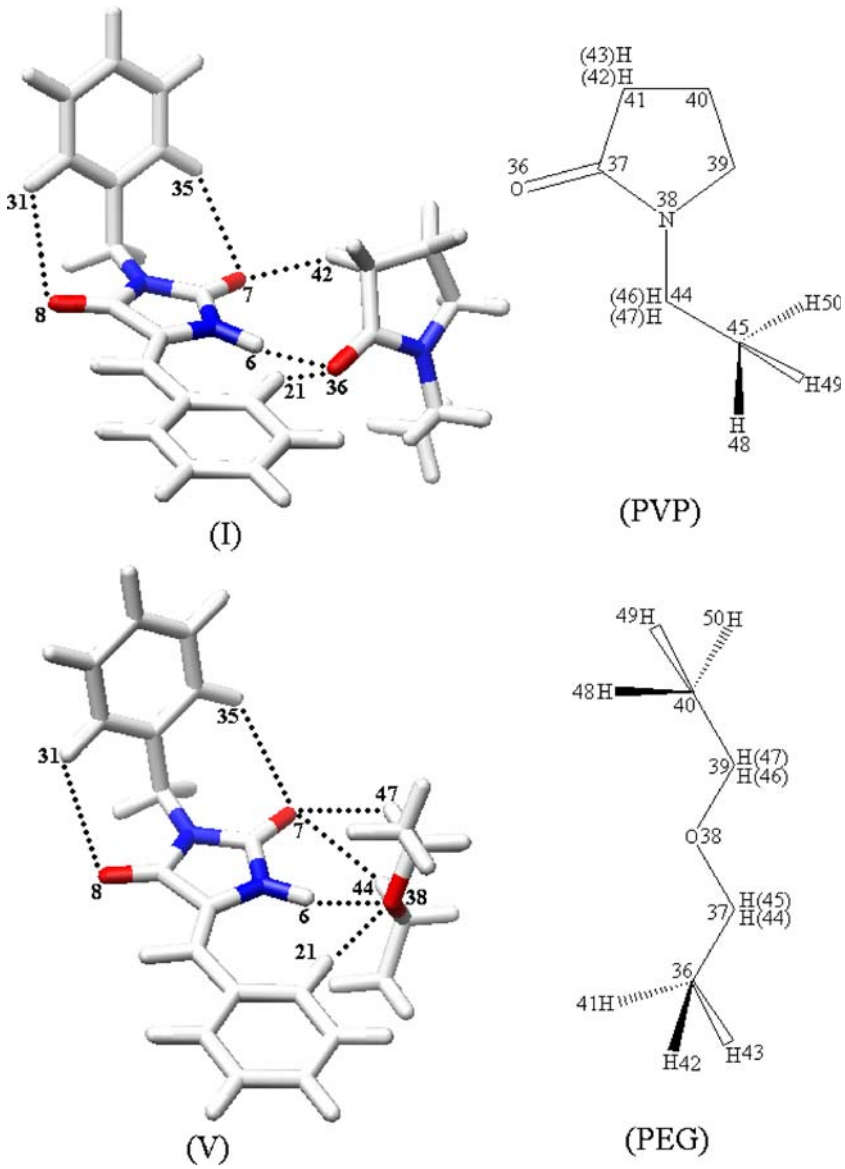

Fig. 2 Optimized geometries of the PVP···1a (I) and PEG···1a (V) complexes using B3LYP/6-31G(d,p) calculations and schematic atomic numbering of PVP and PEG polymers

these vibrational modes are stretching occurring on the hydrogen bond proton donors [50]. According to results of the $\Delta\upsilon$(N–H) red-shifts and $\frac{I(NH),c}{I(NH),i}$ absorption intensity ratios, it is clear that typical hydrogen bonds are formed if the NH bond is the proton donor center. Specifically, we would like to note that complexes (II) and (IV) present the largest $\Delta\upsilon$(NH) red-shifts, with values reaching -341.2 cm^{-1} and -343.1 cm^{-1}, while the greatest absorption intensity ratio of 1006.6 was obtained for (III). It is quite interesting to observe how the infrared spectra of these systems are affected after the formation of the complex [51]. However, after analyzing the chemical shifts on the CH bonds, the results, listed in Table 3, indicate that a blue-shift was verified instead of a red-shift, as observed in recent reports by Ribeiro-Claro *et al*. [52]. Contrary to the NH bond, slight chemical shifts were observed for the CH bond, whose values vary from + 24.6 cm^{-1} to + 35.7 cm^{-1}. When comparing the red-shifts in hydrogen-bonded complexes, where an increase of the absorption intensities for the proton donor bonds is known, it is uncommon that absorption ratios for the blue-shifts present a systematic reduction [53]. However, our results indicate that even though the absorption intensities of the NH modes are increased dramatically, significant reductions in the absorption intensities of the CH bonds were observed, such as in complex (VII), which presented an $\frac{I(CH),c}{I(CH),i}$ ratio of 0.10.

By taking into account the $\Delta\upsilon$(NH) red-shifts and $\frac{I(NH),c}{I(NH),i}$ absorption intensity ratios related to the formation of the ($O_{36}\cdots H_6$) and ($O_{38}\cdots H_6$) hydrogen bonds in complexes (I) and (V), respectively, it would be interesting to examine if the hydrogen bond strength can be explained by these vibrational effects. According to Fig. 3, a satisfactory linear relationship between the NH bond length enhancements, Δr(NH), and their red-shifts, $\Delta\upsilon$(NH), can be observed, and a linear regression coefficient (R^2) of 0.99 was calculated. On the other hand, the ($O_{36}\cdots H_{21}$) and ($O_{38}\cdots H_{21}$) interactions for complexes (I) and (V), respectively, have the opposite behaviour because CH stretch frequencies are shifted to upward values, while the $\frac{I(CH),c}{I(CH),i}$ intensity ratio diminished substantially. In this sense, two distinct types of intermolecular interactions are observed, the traditional red-shift hydrogen bonds and the blue-shifting hydrogen bonds [54, 55].

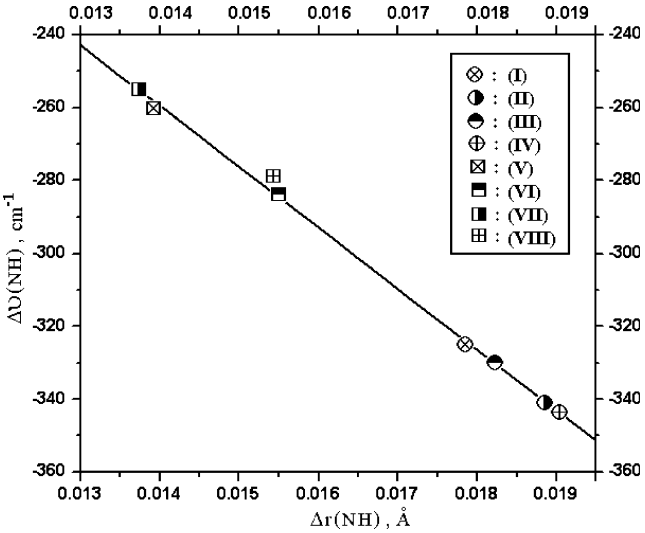

Fig. 3 Relationship between the red-shifts, $\Delta\upsilon$(NH), and bond enhancements, Δr(NH), for the NH bond of the (1a), (2a), (3a) and (4a) isolated molecules upon the formation of the PVP···1a (I), PVP···2a (II), PVP···3a (III), PVP···4a (IV), PEG···1a (V), PEG···2a (VI), PEG···3a (VII) and PEG···4a (VIII) complexes

QTAIM analysis and intermolecular energies

The QTAIM approach and its topological calculations have been used more frequently by theoreticians all over the

Table 3 Vibrational shift modes of **1a**, **2a**, **3a** and **4a** monomers upon the formation of the PVP···**1a** (I), PVP···**2a** (II), PVP···**3a** (III), PVP···**4a** (IV), PEG···**1a** (V), PEG···**2a** (VI), PEG···**3a** (VII) and PEG···**4a** (VIII) complexes using B3LYP/6-31G(d,p) calculations

Molecular systems	Vibrational modes							
	υ(NH)	$\Delta\upsilon$(NH)	I(NH)	$\frac{I(NH),c}{I(NH),i}$	υ(CH)	$\Delta\upsilon$(CH)	I(CH)	$\frac{I(CH),c}{I(CH),i}$
1a	3673.6	–	41.8	–	3212.5	–	16.0	–
2a	3674.2	–	49.6	–	3213.4	–	16.9	–
3a	3676.8	–	48.9	–	3212.0	–	20.3	–
4a	3673.5	–	57.3	–	3213.7	–	21.3	–
(I)	3351.4	−324.9	933.0	22.3	3242.9	+30.4	5.20	0.32
(II)	3333.0	−341.2	866.9	17.5	3238.0	+24.6	12.5	0.74
(III)	3346.6	−330.2	1006.6	20.5	3248.2	+35.7	8.0	0.40
(IV)	3330.4	−343.1	899.6	15.6	3242.4	+28.7	15.5	0.70
(V)	3413.5	−260.1	544.5	13.0	3237.6	+25.1	2.1	0.13
(VI)	3390.4	−283.8	542.7	10.9	3243.8	+30.4	3.4	0.20
(VII)	3421.5	−255.3	572.0	11.6	3244.9	+32.4	2.1	0.10
(VIII)	3394.5	−279.0	571.8	9.9	3248.7	+35.0	4.3	0.20

* Values of υ and I are given in cm^{-1} and $km.mol^{-1}$, respectively

* Values of I(NH), i and I(NH), c mean the absorption intensities of the isolated molecules and the complex, respectively

Table 4 Electronic densities (ρ) and Laplacians ($\nabla^2\rho$) for important interactions in PVP···**1a** (I), PVP···**2a** (II), PVP···**3a** (III) and PVP···**4a** (IV) complexes

BCP	Hydrogen-bonded complexes			
	(I)	(II)	(III)	(IV)
($O_{36}\cdots H_6$)	0.0327 (0.0934)	0.0328 (0.0964)	0.0330 (0.0955)	0.0326 (0.0955)
($O_{36}\cdots H_{21}$)	0.0131 (0.0401)	0.0158 (0.0460)	0.0134 (0.0445)	0.0170 (0.0491)
($H_{42}\cdots O_7$)	0.0122 (0.0372)	– (–)	0.0118 (0.0385)	– (–)
($H_{35}\cdots O_7$)	0.0044 (0.0172)	– (–)	0.0076 (0.0183)	– (–)
($H_{31}\cdots O_8$)	0.0045 (0.0171)	– (–)	– (–)	– (–)
($H_{31}\cdots S_8$)	– (–)	– (–)	0.0048 (0.0169)	– (–)
($H_{46}\cdots O_7$)	– (–)	0.0057 (0.0166)	– (–)	– (–)
($H_{46}\cdots S_7$)	– (–)	– (–)	– (–)	0.0058 (0.0171)
($S_8\cdots H_{23}$)	– (–)	0.0075 (0.0266)	– (–)	0.0079 (0.0243)
($H_{50}\cdots S_7$)	– (–)	0.0029 (0.008)	– (–)	– (–)
($S_7\cdots H_6$)	– (–)	– (–)	– (–)	0.0029 (0.0082)
($S_7\cdots H_{24}$)	– (–)	– (–)	– (–)	0.0073 (0.0227)
($S_8\cdots H_{10}$)	– (–)	– (–)	– (–)	0.0127 (0.0460)

* Values of ρ and $\nabla^2\rho$ (in parenthesis) are given in e/a_0^3 and e/a_0^5, respectively

world [56, 57], in many cases including studies of intermolecular complexes [58] and biological systems [59] that were performed successfully. In this current work, the QTAIM results for complexes (I), (II), (III), and (IV) and complexes (V), (VI), (VII), and (VIII) are presented in Tables 4 and 5, respectively. From QTAIM analysis, results of topological parameters were extracted, including the electronic densities (ρ) and Laplacians ($\nabla^2\rho$). These operators monitor the formation of intermolecular interactions based on depletions and concentrations of charge density. Small ρ and positive $\nabla^2\rho$ values are typically related to intermolecular interactions where the charge density is concentrated on separate nuclei [60]. On the other hand, high and negative values of ρ and $\nabla^2\rho$ suggest that covalent and/or unsaturated bonds are formed. In other words, the charge is concentrated along the pathway of the chemical bond connecting two nuclei through the localization of bond critical points (BCPs) [61]. As is widely known, the QTAIM algorithm integrates the electronic density on a molecular surface, where topological parameters are obtained and used to interpret the chemical stability [62]. For complexes (I), (II), (III), and (IV) and (V), (VI), (VII), and (VIII), QTAIM results indicate the existence of specific interactions between the monomeric units of the PEG and PVP polymers and the imidazolidine derivatives. As seen in Fig. 4, in addition to the ($O_{36}\cdots H_6$) and ($O_{38}\cdots H_6$) hydrogen bonds, another interaction, among the O_{36}, O_{38} and H_{21} atoms, is formed for complexes (I) and (V).

In terms of QTAIM parameters, an examination of the conditions necessary to form secondary interactions can be explained in terms of the electronic density and Laplacian operators. For the electronic densities of the ($O_{36}\cdots H_6$) and ($O_{38}\cdots H_6$) hydrogen bonds in complexes (I), (II), (III), and

Table 5 Electronic densities (ρ) and Laplacians ($\nabla^2\rho$) for important interactions in PEG···**1a** (V), PEG···**2a** (VI), PEG···**3a** (VII) and PEG···**4a** (VIII) complexes

BCP	Hydrogen-bonded complexes			
	(V)	(VI)	(VII)	(VIII)
($O_{38}\cdots H_6$)	0.0307 (0.0802)	0.0308 (0.0791)	0.0303 (0.0791)	0.0289 (0.0755)
($O_{38}\cdots H_{21}$)	0.0105 (0.0322)	0.0105 (0.0322)	0.0114 (0.0345)	0.0154 (0.0434)
($H_{44}\cdots O_7$)	0.0066 (0.0277)	– (–)	0.0066 (0.0229)	– (–)
($H_{47}\cdots S_7$)	– (–)	0.0143 (0.0313)	– (–)	0.0047 (0.0137)
($H_{44}\cdots O_7$)	0.0065 (0.0226)	– (–)	0.0067 (0.0231)	– (–)
($H_{44}\cdots S_7$)	– (–)	0.0142 (0.0310)	– (–)	0.0046 (0.0134)
($H_{35}\cdots O_7$)	0.0040 (0.0159)	– (–)	0.0075 (0.0264)	– (–)
($H_{35}\cdots S_7$)	– (–)	0.0084 (0.0269)	– (–)	0.0075 (0.0226)
($O_8\cdots H_{23}$)	– (–)	– (–)	– (–)	– (–)
($O_8\cdots H_{31}$)	0.0047 (0.0179)	0.0047 (0.0179)	– (–)	– (–)
($S_8\cdots H_{10}$)	– (–)	– (–)	0.0120 (0.0454)	– (–)
($S_7\cdots H_{24}$)	– (–)	– (–)	– (–)	0.0133 (0.049)

* Values of ρ and $\nabla^2\rho$ (in parenthesis) are given in e/a_0^3 and e/a_0^5, respectively

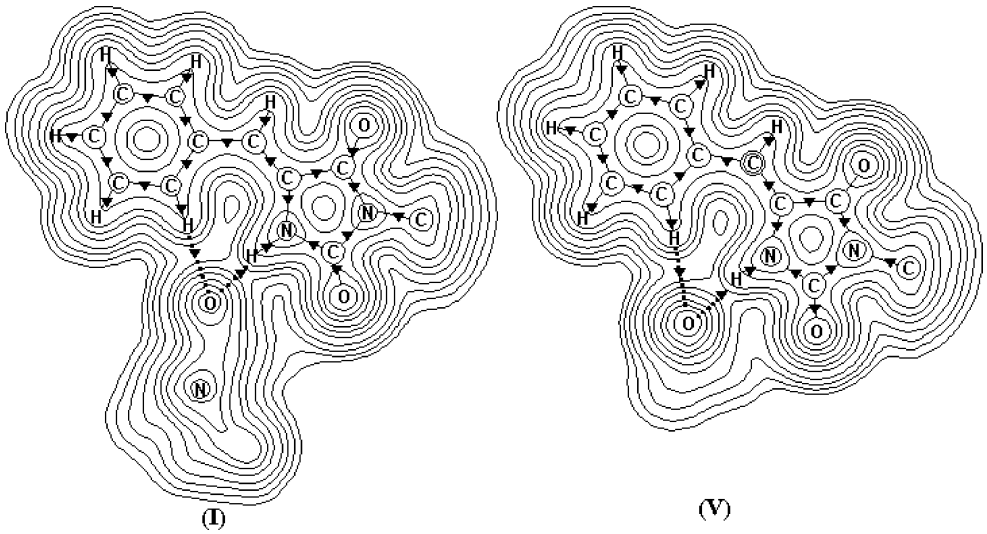

Fig. 4 Line plots of QTAIM electronic density for the PVP···1a (I) and PEG···1a (V) complexes. The black triangles represent BCPs

(IV) and (V), (VI), (VII), and (VIII), the ρ values are in range of 0.0326-0.0330 e/a_0^3 and 0.0289-0.0308 e/a_0^3, respectively. Corroborating data on the hydrogen bond distances, the concentration of charge density on the complexes PVP···**1a-4a** is higher than that observed for the PEG···**1a-4a** complexes. Nevertheless, the (O_{36}···H_{21}) and (O_{38}···H_{21}) blue-shifting hydrogen bonds have charge densities lower than the red-shifting ones, specifically in the range of 0.0131-0.0170 e/a_0^3 for the PVP complexes and 0.0105–0.0154 e/a_0^3 for the PEG systems. Indeed, the interaction of the PVP and PEG units with the NH proton donor (imidazolidine ring) bond is preferred over the formation of the hydrogen-bonded complex, but as suggested here, the blue-shifting hydrogen bonds on the benzylidene ring are also important. In terms of QTAIM concepts, we can confirm that all of the interactions explained above are closed-shell interactions because their Laplacian values are positive. Still, after analyzing the results of the QTAIM calculations, besides the hydrogen bonds and the blue-shifting hydrogen bonds, several secondary and intramolecular interactions were also characterized. For instance, the (H_{42}···O_7), (H_{44}···O_7), and (H_{47}···S_7) hydrogen bonds were examined, and they were formed between the carbonyl and/or thiocarbonyl groups of the imidazolidine ring and the hydrogen atoms of the PVP and PEG units, respectively. These interactions, and other similar ones, are weak hydrogen bonds because low charge density concentrations were quantified. Therefore, significant perturbation in the electronic structure of the PVP···**1a–4a** and PEG···**1a–4a** complexes has not been observed.

However, even though several interactions were identified in PVP···**1a–4a** and PEG···**1a–4a** complexes, it is important to stress that their intermolecular energies are distributed among many intermolecular interactions. By

Table 6 Electronic parameters of **1a**, **2a**, **3a** and **4a** monomers and PVP···**1a** (I), PVP···**2a** (II), PVP···**3a** (III), PVP···**4a** (IV), PEG···**1a** (V), PEG···**2a** (VI), PEG···**3a** (VII) and PEG···**4a** (VIII) complexes using B3LYP/6-31G(d,p) calculations

Complexes	Electronic parameters			
	ΔE	BSSE	ΔZPE	ΔE^C
(I)	53.9	16.5	4.7	32.7
(II)	51.5	14.6	4.5	32.4
(III)	54.3	16.5	4.7	33.1
(IV)	50.5	14.6	4.1	29.3
(V)	39.6	19.7	4.9	15.0
(VI)	37.2	16.6	5.0	15.6
(VII)	39.4	19.6	5.1	14.7
(VIII)	36.0	16.8	5.2	14.0

* Values of ΔE, BSSE, ZPE and ΔE^C are given in kJ mol^{-1}

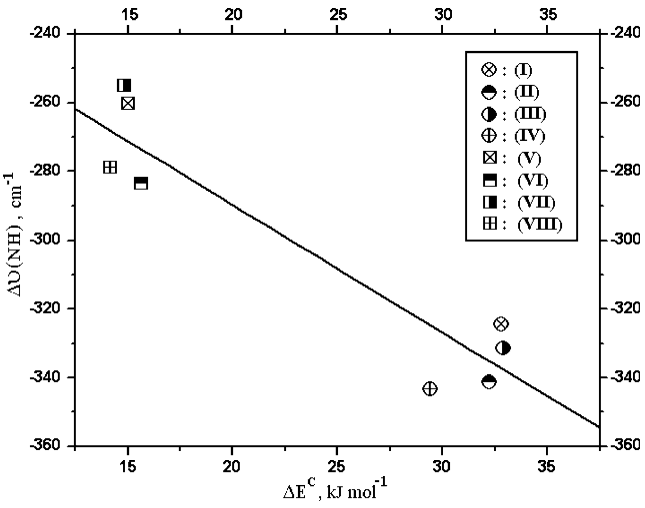

Fig. 5 The relationship between the red-shifts, Δυ(NH), and the intermolecular energies, ΔEC, for the PVP···1a (I), PVP···2a (II), PVP···3a (III), PVP···4a (IV), PEG···1a (V), PEG···2a (VI), PEG···3a (VII) and PEG···4a (VIII) complexes

taking into account the BSSE and ZPE corrections on the uncorrected values of the ΔE hydrogen bond energies, one can finally obtain the results of the ΔE^C corrected hydrogen bond energies for complexes (I), (II), (III), (IV), (V), (VI), (VII) and (VIII), as listed in Table 6. A plot graph illustrated in Fig. 5 shows that a correlation between the Δυ(N–H) red-shifting of the N–H bonds in the **1a**, **2a**, **3a** and **4a** molecules and the ΔE^C corrected hydrogen bonding energies was not successfully obtained. As is widely known in studies of hydrogen complexes, the intermolecular energies and red-shifts are also in full agreement [22–24], but in this work, such a relationship was not observed because the existence of a blue-shift on the C–H center of the benzylidene ring was demonstrated.

Conclusions

In this work, a monomeric model was used to present a theoretical study of the molecular parameters and the ability of imidazolidine derivatives (**1a**, **2a**, **3a** and **4a**) to bind with polyvinylpyrrolidone (PVP) and polyethyleneglycol (PEG) polymers. Based on the structural analysis of the PVP···**1a–4a** and PEG···**1a–4a** hydrogen-bonded complexes at a B3LYP/6–31G(d,p) level of theory, the main deformations on the imidazolidine derivatives and the PVP/PEG systems were measured. It was observed that N–H and C–H bonds of the **1a**, **2a**, **3a** and **4a** imidazolidines were, respectively, increased and decreased upon the formation of the PVP···**1a–4a** and PEG···**1a–4a** hydrogen-bonded complexes. In the infrared spectrum analysis, these effects on the N–H and C–H bonds were characterized as red-shifts and blue-shifts. Although we expected that only the preferential N–H···O red-shifting hydrogen bonds could be formed, it is very interesting that C–H···O blue-shifting hydrogen bonds were also identified.

To complement these results, QTAIM calculations were used to confirm the existence of the N–H···O red-shifting hydrogen bonds and the C–H···O blue-shifting hydrogen bonds. Indeed, calculation of the Laplacian ($\nabla^2\rho$) characterized N–H···O and C–H···O hydrogen bonds as closed-shell interactions ($\nabla^2\rho>0$), whereas N–H and C–H bonds had a shared covalent character ($\nabla^2\rho<0$). Furthermore, in addition to N–H···O and C–H···O interactions, the application of QTAIM localized intramolecular and intermolecular BCPs by which several additional interactions have been identified ($\nabla^2\rho>0$). In summary, formation of the PVP···**1a–4a** and PEG···**1a–4a** hydrogen-bonded complexes is characterized by the existence of many types of interactions, including the N–H···O red-shifting hydrogen bonds and C–H···O blue–shifting hydrogen bonds. Computation of the hydrogen bond energies revealed that PVP···**1a–4a** complexes are more stable than PEG···**1a–4a** ones, with ΔE^C values in the range of 29.3–33.1 kJ.mol^{-1} and 14-15.6 kJ.mol^{-1}, respectively.

Acknowledgments The authors gratefully acknowledge partial financial support from the Brazilian Funding agencies CAPES and CNPq.

References

1. Martin TW, Derewenda ZS (1999) Nature Struct Bio 6:403–406
2. Gancia E, Montana JG, Manallack DT (2001) J Mol Graph Model 19:349–362
3. Hernandes MZ, Leite LFCC, Mourão RHV, Lima MCA, Galdino SL, Neves FAR, Vidal S, Barbe J, Pitta IR (2007) Eur J Med Chem 42:1263–1271
4. Leite ACL, Moreira DRM, Cardoso MVO, Hernandes MZ, Pereira VRA, Silva RO, Kiperstok AC, Lima RS, Soares MBP (2007) Chem Med Chem 2:1339–1345
5. Leite ACL, Lima RS, Moreira DRM, Cardoso MVO, Brito ACG, Santos LMF, Hernandes MZ, Kiperstok AC, Lima RS, Soares MBP (2006) Bioorg Med Chem 14:3749–3757
6. Borg J, Jensen MH, Sneppen K, Tiana G (2001) Phys Rev Lett 86:1031–1033
7. He Y, Zhu B, Inoue Y (2004) Prog Polym Sci 29:1021–1051
8. Wilson AJ (2007) Soft Matter 3:409–425
9. Iliopoulos I, Audebert R (2003) J Poly Sci B: Pol Phys 26:2093–2112
10. Serajuddin ATM (1999) J Pharm Sci 88:1058–1066
11. Craig DQM (2002) Int J Pharm 231:131–144
12. Karavas E, Georgarakis E, Sigalas MP, Avgoustakis K, Bikiaris D (2007) Eur J Pharm Biopharm 66:334–347
13. Teberekidis VI, Sigalas MP (2007) J Mol Struct (THEOCHEM) 803:29-38
14. Warren KS (1978) Gut 19:572–577
15. Albuquerque MCPA, Pitta MGR, Malagueño E, Santana JV, Lima MCA, Pitta IR, Galdino SL (2004) Acta Farm Bon 23:343–348
16. Scholl S, Koch A, Henning D, Kempter G, Kleinpeter E (1999) Struct Chem 10:355–366
17. Baeyer A (1861) Justus Liebigs Ann Chem 119:126–128
18. Oliveira SM, Silva JBP, Hernandes MZ, Lima MCA, Galdino SL, Pitta IR (2008) Quim Nova 31:614–622
19. Karavas E, Georgakakis E, Bikiaris B, Thomas T, Katsos V, Xenakis A (2001) Prog Colloid Polym Sci 118:149–152
20. Hohenberg P, Kohn W (1964) Phys Rev B 136:864–871
21. Kohn W, Sham SJ (1965) Phys Rev A 140:1133–1138
22. Araújo RCMU, da Silva JBP, Ramos MN (1995) Spectrochim Acta A 51:821–830
23. Araújo RCMU, Ramos MN (1996) J Mol Struct (THEOCHEM) 366:233–240
24. Araújo RCMU, Ramos MN (1998) J Braz Chem Soc 9:499–505
25. Nesbitt DJ (1988) Chem Rev 88:843–870
26. Bader RFW (1990) Atoms in molecules. A Quantum Theory. Clarendon, Oxford, UK
27. Oliveira BG, Santos ECS, Duarte EM, Araújo RCMU, Ramos MN, Carvalho AB (2004) Spectrochim Acta A 60:1883–1887
28. Oliveira BG, Duarte EM, Araújo RCMU, Ramos MN, Carvalho AB (2005) Spectrochim Acta A 61:491–494
29. Oliveira BG, Vasconcellos MLAA (2006) THEOCHEM 774:83–88
30. Oliveira BG, Araújo RCMU, Carvalho AB, Lima EF, Silva WLV, Ramos MN, Tavares AM (2006) THEOCHEM 775:39–45
31. Oliveira BG, Pereira FS, Araújo RCMU, Ramos MN (2006) Chem Phys Lett 433:390–394

32. Oliveira BG, Araújo RCMU, Carvalho AB, Ramos MN (2007) Spectrochim Acta A 68:626–631
33. Oliveira BG, Araújo RCMU, Carvalho AB, Ramos MN (2007) J Theor Comp Chem 6:647–660
34. Oliveira BG, Pereira FS, Araújo RCMU, Ramos MN (2006) Chem Phys Lett 427:181–184
35. Oliveira BG, Araújo RCMU, Chagas FF, Carvalho AB, Ramos MN (2008) J Mol Model 14:949–955
36. Oliveira BG, Araújo RCMU, Carvalho AB, Ramos MN (2009) J Mol Model 15:123–131
37. Oliveira BG, Vasconcellos MLAA, Olinda RR, Filho EBA (2009) Struct Chem 20:81–90
38. Frisch MJ, Trucks GW, Schlegel HB, Scuseria GE, Robb MA, Cheeseman JR, Montgomery JA Jr, Vreven T, Kudin KN, Burant JC, Millam JM, Iyengar SS, Tomasi J, Barone V, Mennucci B, Cossi M, Scalmani G, Rega N, Petersson GA, Nakatsuji H, Hada M, Ehara M, Toyota K, Fukuda R, Hasegawa J, Ishida M, Nakajima T, Honda Y, Kitao O, Nakai H, Klene M, Li X, Knox JE, Hratchian HP, Cross JB, Adamo C, Jaramillo J, Gomperts R, Stratmann RE, Yazyev O, Austin AJ, Cammi R, Pomelli C, Ochterski JW, Ayala PY, Morokuma K, Voth GA, Salvador P, Dannenberg JJ, Zakrzewski VG, Dapprich S, Daniels AD, Strain MC, Farkas O, Malick DK, Rabuck AD, Raghavachari K, Foresman JB, Ortiz JV, Cui Q, Baboul AG, Clifford S, Cioslowski J, Stefanov BB, Liu G, Liashenko A, Piskorz P, Komaromi I, Martin RL, Fox DJ, Keith T, Al-Laham MA, Peng CY, Nanayakkara A, Challacombe M, Gill PMW, Johnson B, Chen W, Wong MW, Gonzalez C, Pople JA (2004) GAUSSIAN 03, Revision B.04. Gaussian Inc, Wallingford, CT
39. Ren FD, Cao DL, Wang WL, Ren J, Hou SQ, Chen SS (2009) J Mol Model 15:515–523
40. Kolboe S, Svelle S (2008) J Phys Chem A 112:6399–6400
41. Yılgör E, Yılgör İ, Yurtsever E (2002) Polymer 43:6551-6559
42. Cioslowski J (1993) Chem Phys Lett 203:137–142
43. Cioslowski J (1992) Chem Phys Lett 194:73–78
44. Cioslowski J, Surjan PR (1992) THEOCHEM 255:9–33
45. AIM 2000 1.0 program designed by Biegler-König F, University of Applied Sciences, Bielefeld, Germany
46. van Duijneveldt FB, Murrell JN (1967) J Chem Phys 46:1759–1767
47. McQuarrie DA (1973) Statistical thermodynamics. Harper and Row, New York
48. Boys SB, Bernardi F (1970) Mol Phys 19:553–566
49. Pauling L (1945) The nature of the chemical bond. Cornell University Press, Ithaca
50. Kovács A, Varga Z (2006) Coord Chem Rev 250:710–727
51. Herrebout WA, Delanoye SN, van der Veken BJ (2004) J Phys Chem A 108:6059–6064
52. Marques MPM, da Costa AM Amorim, Ribeiro-Claro PJA (2001) J Phys Chem A 105:5292–5297
53. Barnes AJ (2004) J Mol Struct 704:3–9
54. Cubero E, Orozco M, Hobza P, Luque FJ (1999) J Phys Chem A 103:6394–6401
55. Špirko V, Hobza P (2006) Chem Phys Chem 7:640–643
56. Grabowski SJ (2005) Hydrogen bonds–new insights. Springer, Berlin
57. Matta CF, Boyd RJ (2007) The quantum theory of atoms in molecules. Wiley, Weinheim
58. Wu DL, Liu L, Liu GF, Jia DZ (2007) J Phys Chem A 111:5244–5252
59. Filho EBA, Ventura E, do Monte SA, Oliveira BG, Junior CGL, Rocha GB, Vasconcellos MLAA (2007) Chem Phys Lett 449:336–340
60. Bader RFW (2005) Monatshefte für Chemie 136:819–854
61. Bader RFW (1985) Acc Chem Res 18:9–15
62. Bader RFW (1998) J Phys Chem A 102:7314–7323